Nuclear Instruments and Methods in Physics Research A 1070 (2025) 170035

Contents lists available at ScienceDirect

Nuclear Inst. and Methods in Physics Research, A

journal homepage: www.elsevier.com/locate/nima

Radiation characterization of SiPMs for HERD PSD

Yirong Zhang [a], Yaqing Liu [b,c], Jifeng Han [a], Dongya Guo [b,c], Yongwei Dong [b,c], Min Gao [b,c], Ruirui Fan [b,d,e], Zhixin Tan [b,d], Zhigang Wang [b,c,e,*], HERD PSD Collaboration

[a] Key Laboratory of Radiation Physics and Technology of the Ministry of Education, Institute of Nuclear Science and Technology, Sichuan University, Chengdu, 610064, China
[b] Institute of High Energy Physics, Chinese Academy of Sciences, Beijing, 100049, China
[c] Key Laboratory of Particle Astrophysics, Chinese Academy of Sciences, Bejing, 100049, China
[d] Spallation Neutron Source Science Center, Dongguan, 523803, China
[e] State Key Laboratory of Particle Detection and Electronics, Bejing, 100049, China

ARTICLE INFO

Keywords:
HERD
PSD
SiPM
Radiation damage
Dark current
Annealing

ABSTRACT

Silicon photomultipliers (SiPMs) have been used in several space-borne missions, and the radiation effect as well as the performance degradation must be a concern during space operations. SiPMs will be used as photon-electric devices of the Plastic Scintillator Detector (PSD) for the High Energy Cosmic Radiation Detection (HERD) facility, and the performance change of these SiPMs under in-orbit radiation needs to be studied to satisfy the 10 years of in-orbit operation mission. In this study, the radiation damage and annealing for potential SiPM candidates including Hamamatsu and Novel Device Laboratory series have been done. The dark current for S14160–3010 PS (HM10), S14160–3015 PS(HM15), and EQR1511-3030D-S(NDL15) was observed to increase by a factor of 300, 400, and 200 after exposure to an equivalent on-orbit dose of 10 years. PSD showed a significant decrease in MIP detection capability after irradiation. In addition, annealing of neutron radiation damages in SiPM at temperatures 50 °C and room temperature is studied.

1. Introduction

The High Energy Cosmic-Radiation Detection (HERD) facility, which is an international collaboration project by China, Italy, Switzerland, and Spain, is a large-scale space experiment on particle detection that will be onboard China's Space Station around 2027. The main scientific goals of HERD are.

- Searching for the decay or annihilation signal from dark matter by measuring the energy spectra and anisotropy of high energy electrons and gamma-rays;
- Studying the origin, propagation, and acceleration mechanism of cosmic rays by measuring precisely and directly the energy spectra and composition of primary cosmic rays from 10 GeV up to a few PeV;
- Monitoring the high energy gamma-ray sky from 0.5 GeV to 100 TeV [1].

The PSD is a sub-detector of HERD, particularly operated as an anti-coincidence detector to discriminate incident photons from charged particles, and is capable of providing precise charge measurement of incoming cosmic–ray nuclei in the range of Z = 1–28 of atom number.

The PSD will consist of plastic scintillator bars coupled to SiPMs [2]. The choice has been driven by recent SiPM technological developments that demonstrate: fast light signal detection; good sensitivity to low light yields; lower power consumption and robustness[3–6]. These features delineate the practicality and versatility of SiPMs in space applications, whereas PMTs require well–increased operation voltages (~kV) and large size, therefore not optimized for HERD PSD. Moreover, plastic scintillators featuring low density and good radiation hardness, while being affordable and available in mass production, seem as a suitable choice regarding the PSD realization. Many other tests are studying plastic scintillators coupled to the SiPMs for space missions, including the Gamma-Ray Integrated Detectors (GRID) [7], e-Astrogam [8], and AMEGO [9].

The degradation of SiPM in orbit has an important impact on the performance of PSD. Irradiation damage is one of the main drawbacks restricting the application of SiPM in space [10,11]. Therefore, a

* Corresponding author. Institute of High Energy Physics, Chinese Academy of Sciences, Beijing 100049, China.
E-mail address: wangzhg@ihep.ac.cn (Z. Wang).

https://doi.org/10.1016/j.nima.2024.170035
Received 5 April 2024; Received in revised form 17 October 2024; Accepted 29 October 2024
Available online 4 November 2024
0168-9002/

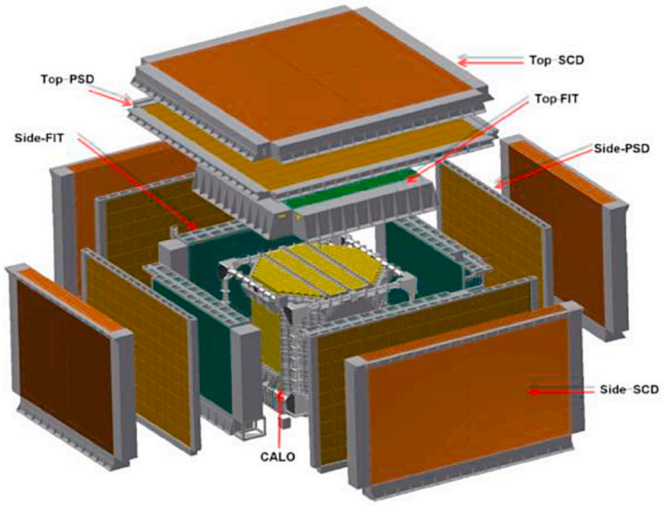

Fig. 1. The layout of HERD.

Table 1
SiPM equivalent proton fluence and neutron fluence with 2 times margin and different shielding thicknesses after 10 years of operation (solar minimum).

Shield thickness	0.0001 mm	3 mm
Equivalent 10 MeV proton n_{eq}/cm^2	2.29E10	5.46E09
Equivalent 1 MeV neutron n_{eq}/cm^2	9.13E10	2.18E10

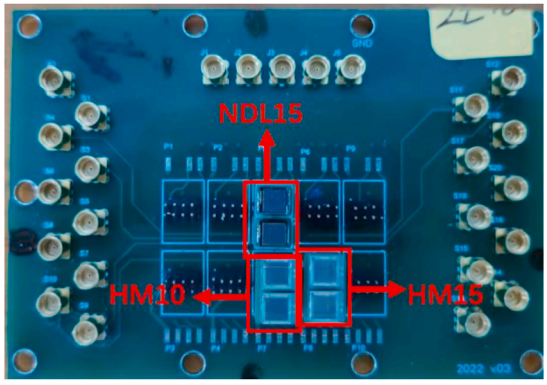

Fig. 2. The test circuit boards.

strategy for radiation damage of SiPM is required. Annealing is a well-established method for addressing SiPM performance recovery against radiation damage. It has previously been observed that long-time annealing at both room temperature [12,13] and a high temperature [14–17] can effectively restore the performance of SiPM.

2. Flux range calculation

In this section, the calculation of on-orbit equivalent proton intensity and the estimation of equivalent neutron fluence of HERD SiPM is introduced.

The radiation dose of the SiPM operating space environment was estimated. HERD will be installed on board the Chinese Space Station (CSS) around 2027, following a Low-Earth Orbit (LEO) at an altitude of approximately 400 km and an inclination angle of 42°, and the expected life span is $\geq$ 10 years [18]. PSD is located on the periphery of HERD, and the outer layer has only Silicon charge detectors(SCD), as shown in Fig. 1. The equivalent aluminum shielding thickness of PSD SiPM can be estimated within 1–3 mm, so the fluence calculation is based on 3 mm Al shield thickness and without shielding.

In our study, a typical satellite orbit was considered: 400 km 42° inclination (circular Low Earth Orbits, Polar). The expected proton fluence along this orbit was estimated through the use of SPENVIS software, for a ten-year mission with minimum solar activity. SPENVIS provided as output the spectra of total mission average flux and total mission fluence related to several contributions: protons and electrons trapped into the terrestrial magnetic field [19].

In space, proton irradiation is predominant, but due to CSNS limitations, neutron irradiation is performed for SiPMs. Radiation damage in SiPMs includes bulk damage from Non-Ionizing Energy Loss (NIEL) and surface damage from Ionizing Energy Loss (IEL). Low-energy photons and electrons mainly cause surface damage, while high-energy particles cause significant bulk damage. This study focuses on high-energy electron and proton irradiation, where surface damage is negligible compared to displacement damage [20]. To compare the displacement damage of different particles, equivalent 10 MeV protons are converted to 1 MeV neutrons using NIEL coefficients [21,22]. Referring to the NIEL data of neutrons and protons in Si calculated by SEEAP, the NIEL coefficient for 1 MeV neutrons in Si material is 1.97E3 MeV/cm^{-2}/g, and for 10 MeV protons, it is 7.86E3 MeV/cm^{-2}/g. If the fluence of 10 MeV protons is set to 2.29E11 n_{eq}/cm^2, the equivalent fluence for 1 MeV neutron is 9.13E11 n_{eq}/cm^2, as shown in Table 1.

3. Experimental setup

To study radiation damage on SiPM with a small pitch size ($\leq$ 15 μm), some SiPM from two manufacturers was measured. The HAMAMATSU S14160–3015 PS(HM15), S14160–3010 PS(HM10) and NDL EQR1511-3030D-S(NDL15)SiPMs feature pitches of 15 μm,10 μm and 15 μm, respectively. They are installed on the circuit board, as shown in Fig. 2. This irradiation experiment will mainly compare the performance of SiPM pre- and post-irradiation.

The SiPMs were irradiated at the China Spallation Neutron Source (CSNS) in July 2022 by using the ES #2 spot, as shown in Fig. 3(a). Back-streaming neutrons through the incoming proton channel at the spallation target station of CSNS has been exploited as a white neutron beamline (so-called Back-n). The intensity of the neutron beam is in the order of 5.0 × 10^6 n/cm^2/s at 80 m from the target and has an excellent energy spectrum spanning from 1 MeV to 100 MeV [23]. In this experiment, the neutron beam was used to irradiate SiPM from 10E9 to 10E12 n_{eq}/cm^2.

In addition, NDL15 SiPMs were irradiated at Sichuan University using the 3 MV Tandem Accelerator. A 3 MeV proton beam is used to bombard the tritium target, where neutrons are generated through nuclear reactions, and the neutron energy in the 0° direction is about 2.3 MeV [24,25]. The SiPM to be irradiated is placed in the direction of 0°, approximately 7 cm away from the neutron target, as shown in Fig. 3(b). During this neutron irradiation, the neutron fluence rate on the SiPM circuit board was about 3.3E7 cm^{-2}/s. The NDL15 SiPMs have been irradiated with neutrons, corresponding to a neutron fluence of 4.6E10 n_{eq}/cm^2 and 1.35E12 n_{eq}/cm^2, respectively. The SiPM used in the experiment and the neutron irradiation fluence in CSNS and SCU are shown in Table 2.

4. Experiment results

The performance of SiPM before and after the irradiation experiment is studied, and then the performance after annealing is discussed in this section. The current-voltage (I–V) characteristics and dark count rate are monitored before and after irradiation. Then, the performance of the PSD prototype using the irradiated SiPM was analyzed, SNR_{mip} and RES_{mip} of the MIP were quantitatively analyzed. As for the annealing experiment, the performance after room-temperature annealing and high-temperature annealing (50 °C) are reported. Finally, based on the irradiation results and annealing results, a method of conducting on-

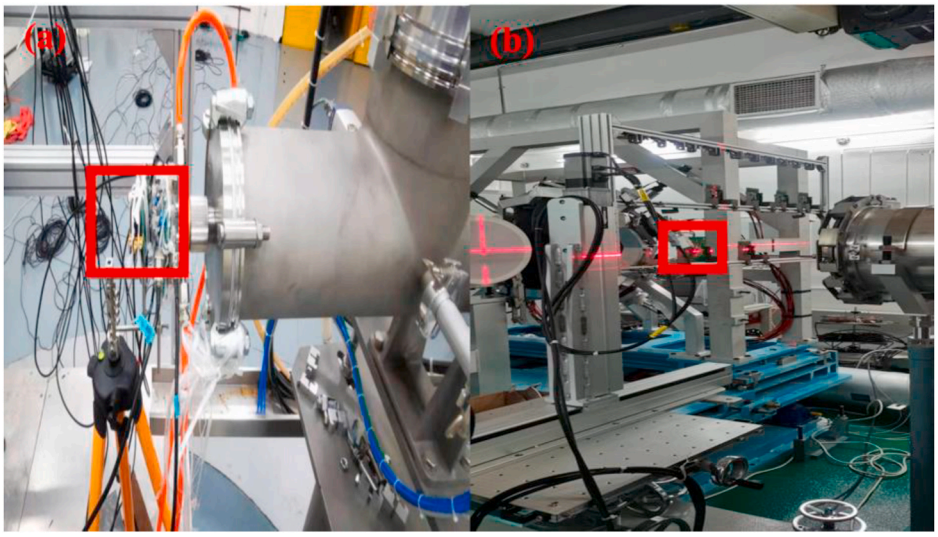

Fig. 3. China Spallation Neutron Source (CSNS)(a) and 3 MV Tandem Accelerator in Sichuan University(b). The test circuit boards are shown in the red box.

Table 2
Introduction of SiPMs.

Irradiation site(Fluence [n_{eq}/cm^2])	Manufacturer	Model	Pixel Size	Operational Voltage	Abbreviation
CSNS	Hamamatsu	S14160–3015 PS	15 μm	43 V	HM15
1E9(0.5-year 3 mm Al shield) 5E9(2.5-year 3 mm Al shield)	Hamamatsu	S14160–3010 PS	10 μm	42 V	HM10
1E10(5-year 3 mm Al shield) 2E10(10-year 3 mm Al shield) 5E11(5-year unshielded) 1E12(10-year unshielded)	NDL	EQR1511-3030D-S	15 μm	37 V	NDL15
SCU 4.6E10(20-year 3 mm Al shield) 1.35E12(10-year unshielded)	NDL	EQR1511-3030D-S	15 μm	37 V	NDL15

orbit thermal annealing for five days per year was proposed.

4.1. I–V characteristics analysis after irradiation

The effect of the irradiation on the dark current of the SiPMs was measured. The I–V characteristics were measured utilizing the Keithley 2450 Source Measurement Unit before and after irradiation. The voltage range was set across the 25–50 V spectrum for the Hamamatsu and NDL SiPMs. The increase of dark current for SiPMs (HM10, HM15, NDL15) is reported in this paper. The increase in dark current leads to a decrease in signal-to-noise ratios, degrading the performance of PSD [26].

Fig. 4(a), (b), and (c) show I–V characteristics for three different SiPM series: HM10, HM15, and NDL15. Due to the Typical Breakdown Voltage of HM10, HM15, and NDL15 being 38V, 38V, and 30V respectively, the voltage was scanned in the range of 25V–50V during the measurement of the I–V curves. Their on-orbit currents for 1 and 10 years are shown in Table 3. After 10 years in orbit, the currents for NDL15, HM10, and HM15 have increased to 200, 300, and 400 times their initial currents, respectively.

4.2. Current increase versus neutron fluence

The effects of different neutron fluences on HM and NDL series SiPMs were studied. By subtracting pre-irradiation currents from post-irradiation currents, a relationship between current increase and neutron fluence was reported, as shown in Fig. 5. For all series of SiPM, as the neutron fluence increases, the dark current increases.

The larger the pixel, the greater the current increase rate of the SiPM. For irradiation fluences below 2E10, the increase rate in SiPM current within the same cell exhibits consistency which can be seen from the current increase of HM15 and NDL15. For irradiation fluences over 5E11, the linear slope of the current increase displays a difference.

The current increase of HM15 was 1.49 times that of HM10. It can be seen that for the same pixel size of 15 μm, the current increase of NDL15 is larger than that of HM15.

4.3. DCR analysis for NDL series

Dark count rate(DCR) has been measured at different voltages and different temperatures (−20,0,10,20,25,30 °C) for NDL15 with 5-year on-orbit dose irradiation. The relationship of DCR is obtained by the same procedure as previous literature [27].

According to Fig. 6, lower DCR can be attained by lowering the temperature. The temperature dependence rises proportionally, exhibiting an increase of 1.5 times for every 10 °C in irradiated specimens. In addition, Lower DCR can be attained by lowering the overvoltage, although this reduces PDE and gain.

4.4. Comparision of MIP detection

The cosmic ray test is designed to explore the damage of space radiation to the PSD detector, which provides some reference for the in-orbit operation of HERD.

The cosmic ray testing system built in the laboratory is shown in Fig. 7. The test system contains two trigger modules, which can trigger cosmic rays muons that vertically penetrate the plastic scintillator. An EJ-200 plastic scintillator with dimensions of 100 mm × 100 mm x 5 mm was coupled to.

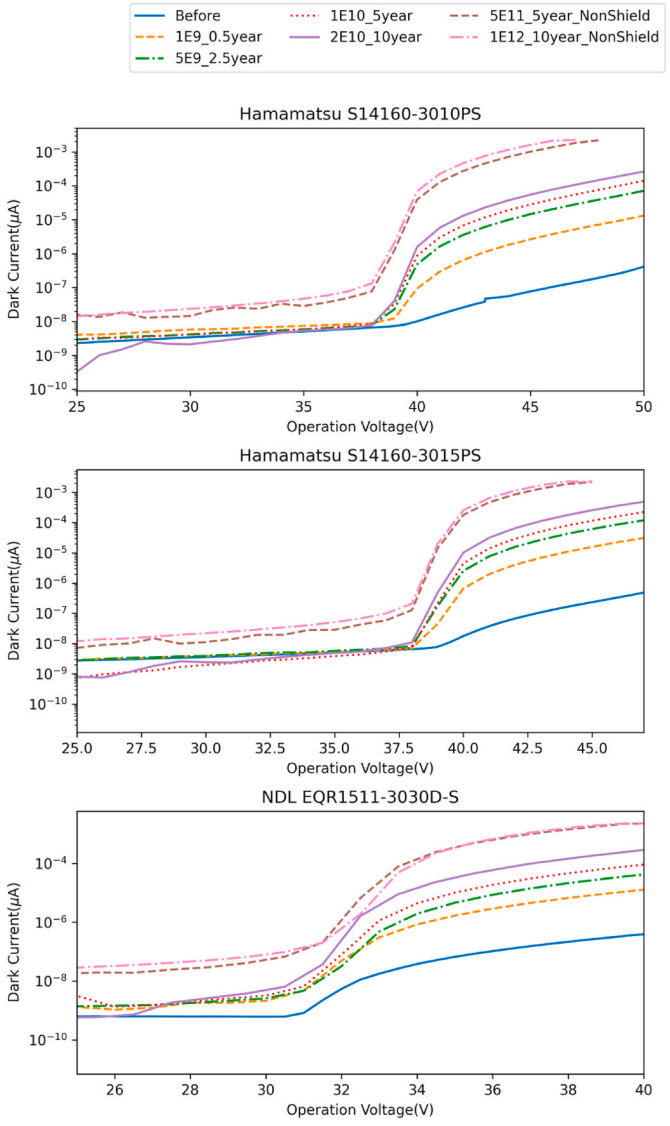

Fig. 4. Current-Voltage curve measured at room temperature (25 °C) of different SiPM (a), Hamamatsu S14160–3010 PS SiPM with 10 μm cell pitch and (b) Hamamatsu S14160–3015 PS SiPM with 15 μm cell pitch and (c) NDL EQR1511-3030D-S with 15 μm cell pitch at different irradiation fluences.

Table 3
Current increase for 1 and 10 years in orbit.

Model	Current(Not irr)	Current (1 year on-orbit)	Current (10 years on-orbit)
NDL15	150 nA	4.5 μA	30 μA
HM10	40 nA	1.2 μA	12 μA
HM15	70 nA	4 μA	30 μA

SiPMs to collect photons at room temperature (25 °C). Four SiPMs were used, including NDL15 and HM15 before and after irradiation, as shown in Fig. 6, operating at the overvoltages 8 V for NDL15, and 4 V for HM15.

Fig. 8 shows the MIP and pedestal which were obtained by integration of SiPM measured waveforms by four SiPMs. In Fig. 8(a)(b)(c)(d), the orange line represents the pedestal fitted with the Gaussian function, the red line represents the MIP fitted with a convoluted Landau and Gaussian function, the detection efficiency of MIP is largely determined by SNR_{mip}. To study the impact of irradiation on detection efficiency,

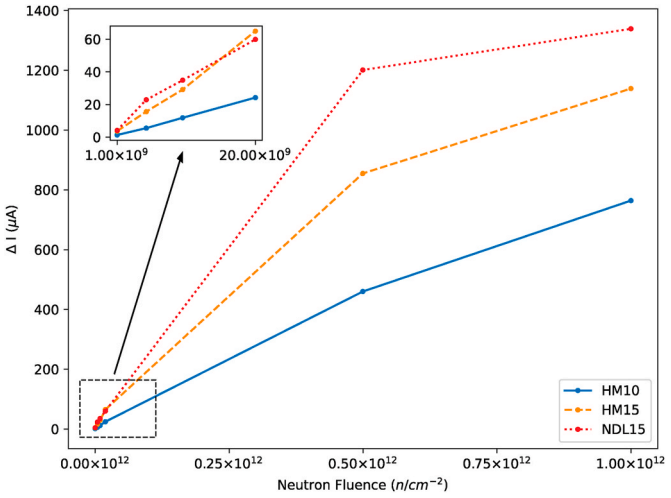

Fig. 5. A relationship between current increase and neutron fluence from 1E9 n_{eq}/cm^2 to 1E12 n_{eq}/cm^2 for four SiPMs, that is HM10, HM15, NDL6, and NDL15.

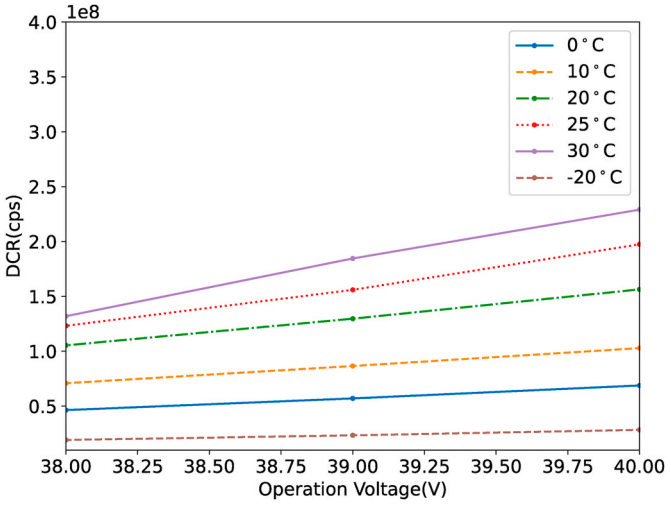

Fig. 6. Dcr of NDL15 from −20 °C to 30 °C.

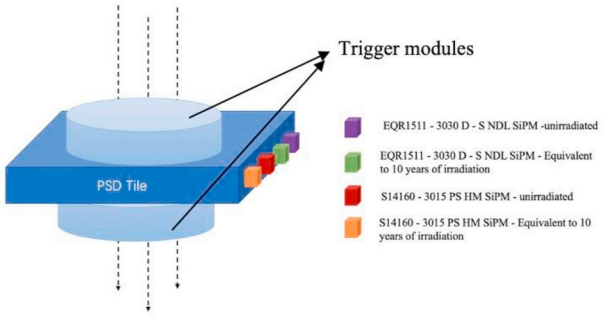

Fig. 7. The cosmic ray test system, including two trigger modules and the EJ-200 plastic scintillator coupled with four SiPMs.

SNR_{mip} of the MIP is defined as Formula (1).

$$SNR_{mip} = \frac{RMP - PMean - 2.5 \times PSigma}{FWHM/2.355} \quad (1)$$

Where RMP represents the peak position of the MIP. FWHM is the full

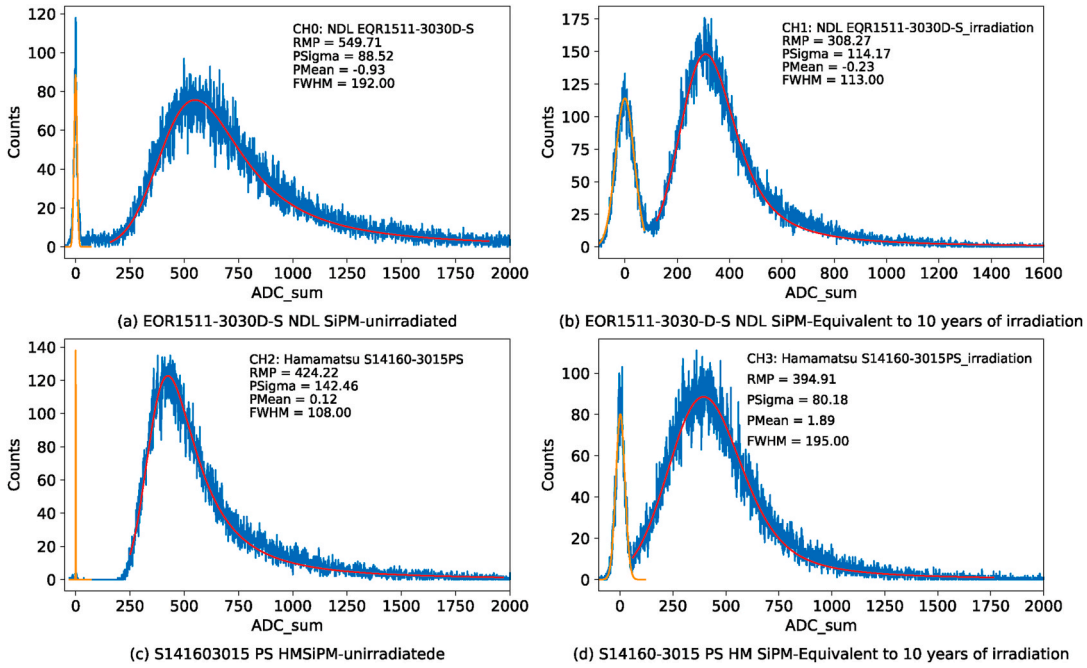

Fig. 8. The MIP and pedestal measured by NDL15 and HM15 when coupled with the PSD. (a) measured by NDL15 before irradiation. (b) measured by NDL15 SiPM after irradiation. (c) measured by HM15 before irradiation. (d) measured by HM15 after irradiation. The orange line represents the MIP fitting, and the green line represents the pedestal fitting. SiPM are numbered by channel No. ((a)-CH0, (b)-CH1,(c)-CH2,d-(CH3)).

Table 4
the SNR_{mip} and RES_{mip} before and after irradiation.

SiPM Manufacturers	before irradiation		after irradiation	
	SNR_{mip}	RES_{mip}	SNR_{mip}	RES_{mip}
HM S14160-3015 PS	2.04	25.4%	0.52	49.6%
NDL EQR1511-3030D-S	1.52	33.6%	1.18	35.5%

width at half maximum of the Landau convolution Gaussian function. PMean represents the mean given by fitting the pedestal using a Gaussian function. PSigma represents the standard deviation given by pedestal fitting using the Gaussian function. According to Formula (1), SNR_{mip} of the MIP measured by the NDL15 and HM15 SiPM before and after irradiation are shown in Table 4. It can be seen that SNR_{mip} of the MIP becomes worse after irradiation, SNR_{mip} of MIP of the PSD decreases by 74.5%, from 2.04 to 0.52 for HM15, and by 22.3%, from 1.52 to 1.18 for NDL15 after irradiation.

In terms of charge measurement, RES_{mip} of MIP is defined as Formula (2).

$$RES_{mip} = \frac{FWHM}{RMP - PMean} \tag{2}$$

According to Formula (2), RES_{mip} of the SiPM measured MIP before and after irradiation are shown in Table 4. It can be seen that the RES_{mip} of MIP becomes worse after irradiation, from 25.4% to 49.6% for HM15 and from 33.6% to 35.5% for NDL15.

4.5. Annealing analysis

SiPMs have been irradiated with white light neutron beams at CSNS, and also with monoenergetic neutron irradiation at the Sichuan University tandem accelerator.

4.5.1. White-neutron annealing result

The relationship between the increase of dark current and the overvoltage after irradiation was obtained to study the annealing at room temperature after white light neutron(Beams of neutrons with a continuous energy distribution)irradiation. Fig. 9 summarizes the data obtained for NDL15, HM15, and HM10 in fluence of 1E9 n_{eq}/cm^2. Taking into account the I–V characteristics, the annealing effect for different overvoltages is consistent.

Fig. 10 shows the annealing rates of HM10, HM15, and NDL15 began to become slow after a few (4–5) days. On the 10th day, the dark current is reduced to up to 20% of its original value. In addition, we observe that a higher irradiation dose correlates with a faster annealing rate for the SiPM.

4.5.2. Monoenergetic neutron irradiation annealing result

In addition to studying the annealing after white light neutron irradiation, the annealing study after monoenergetic neutron irradiation was conducted.

According to Fig. 11(a), the dark current of NDL15 is reduced by 18% after five days of annealing at 50 °C after irradiating in neutron fluences of 1.35E12 n_{eq}/cm^2. There is a fast recovery of the current in the first five days at 50 °C annealing. The recovery trend slows down after the first five days. After 38 days of annealing, the current is reduced by 25%.

At room temperature with neutron fluences of 4E10 n_{eq}/cm^2(close to the ten-year dose under 3 mm Al shielding), as shown in Fig. 11(b), the annealing decreased by 12% after the first 5 days, the annealing decreased by 27% after the first 11 days. There is a fast recovery of the current in the first 11 days at room temperature.

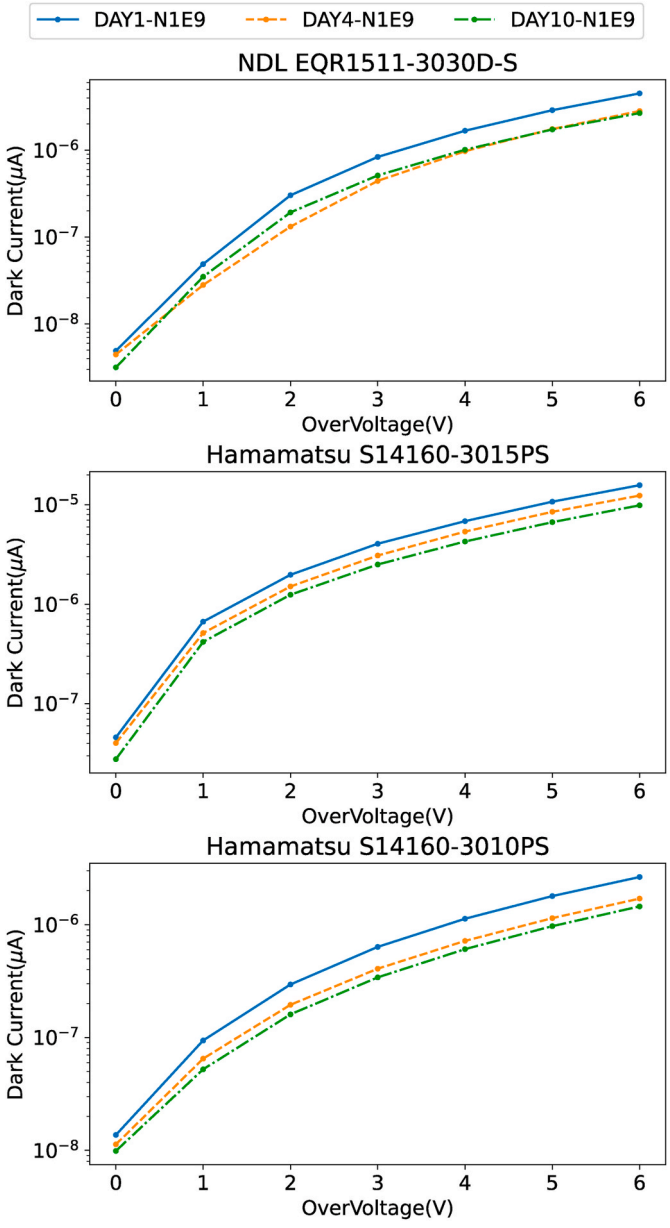

Fig. 9. Dark Current (μA) measured for NDL EQR1511-3030D-S, Hamamatsu S14160–3015 PS, and Hamamatsu S14160–3010 PS on Day 1, Day 4, and Day 10 after exposure to a neutron fluence of 1E9 at room temperature.

Results from other literature indicate the annealing effect is more efficient at high temperatures [28]. Considering the softening point of the EJ-200 plastic scintillator(75 °C) and faster annealing rate at higher temperatures in the short term, the annealing temperature(50 °C) is recommended in the HERD project. During on-orbit operations, it is crucial to achieve the annealing effect promptly to maximize effective detection time.

5. Conclusion and discussion

For a single SiPM, considering two times margin, the dark current for

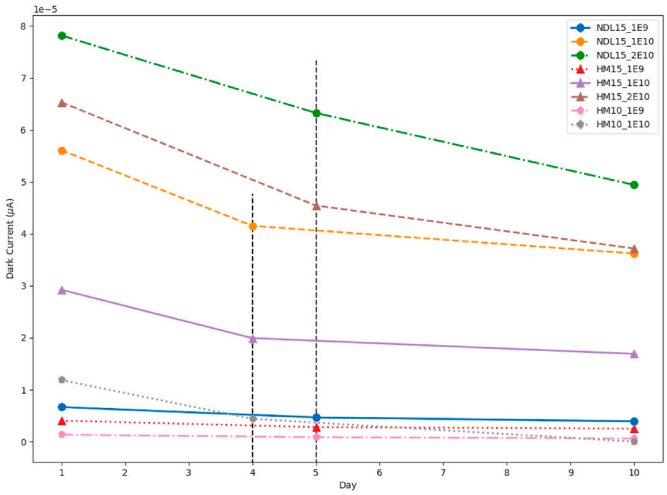

Fig. 10. Dark current of SiPM at room temperature annealing. The operating voltage is 43 V for HM10, 42 V for HM15, and 37 V for NDL15. The irradiation fluence to each HM15 and NDL15 SiPM were 1E9,5E9,1E10,2E10 n_{eq}/cm^2. The irradiation fluence to HM10 SiPM were 1E9,5E9,1E10 n_{eq}/cm^2.

Hamamatsu with 15 μm pixels increases by 400 times to 30 μA exposed to a 3 mm Al shielded environment with a 10-year dose. The dark current for NDL with 15 μm pixels increased by 200 times to 30 μA, and the dark current for HM with 10 μm pixels increased by 300 times to 12 μA. For a SiPM with a pixel size of 15 μm, the dark noise of Hamamatsu is lower than that of NDL, the initial current of NDL is half of that of Hamamatsu, and the currents of the two are of the same magnitude after irradiation. For Hamamatsu manufacturers, the anti-radiation performance of HM with 10 μm pixels is better than HM with 15 μm pixels.

Cosmic ray muons test results show that when SiPMs are irradiated, the charge resolution ability and detection efficiency of PSD become worse.

The results of annealing experiments show that annealing has a faster recovery on detections in high temperatures. Considering the soft point of plastic scintillators(75 °C), 50 °C is a reasonable annealing temperature. The working temperature of PSD is controlled at around 0 °C, so the recovery of SiPM after radiation damage was tentatively promoted by thermal annealing with a hot plate [29]. Considering that the first five days of high-temperature annealing(50 °C) are the fastest annealing stage, we suggest stopping on-orbit operation for 5 days every year to perform thermal annealing. In this case, we predict the trend of dark current in orbit considering that the irradiation and annealing processes are carried out simultaneously, which is a complex process with multiple variables coupled together. The predicting result shows that heating the sensors for 5 days after 1 year of operation for HERD would suffice to reduce the current increase by a factor of 2.

Considering ten years of on-orbit measurements without shielding, the total power consumption of 8000 SiPMs will rise to 403.2W, 275.2W, 395.2W for HM15, HM10 and NDL15 under recommended operation voltage (42V for HM15, 43V for HM10, 37V for NDL15) without considering annealing. This requires PSD not only to operate in low-temperature environments, but also to reserve sufficient margin in power supply design.

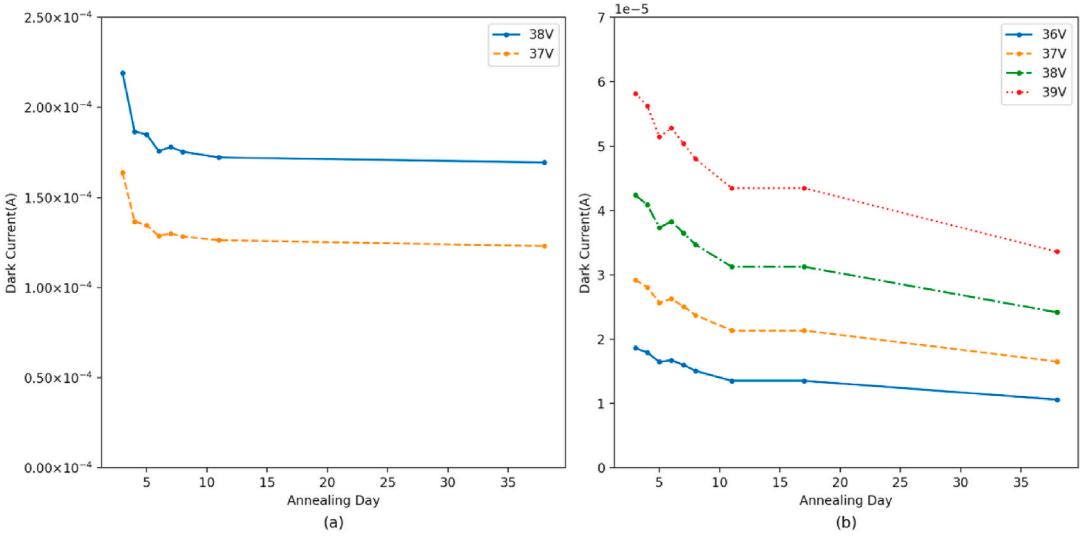

Fig. 11. Dark current of NDL15 SiPM at (a) 50 °C and (b) room temperature annealing.

CRediT authorship contribution statement

Yirong Zhang: Writing – review & editing, Writing – original draft, Software, Formal analysis. **Yaqing Liu:** Writing – review & editing, Investigation, Data curation, Conceptualization. **Jifeng Han:** Writing – review & editing, Investigation, Conceptualization. **Dongya Guo:** Investigation. **Yongwei Dong:** Investigation. **Min Gao:** Investigation. **Ruirui Fan:** Investigation. **Zhixin Tan:** Investigation. **Zhigang Wang:** Writing – review & editing, Validation, Methodology, Investigation, Funding acquisition, Data curation, Conceptualization.

Declaration of competing interest

The authors declare that they have no known competing financial interests or personal relationships that could have appeared to influence the work reported in this paper.

Acknowledgment

This work is supported by the National Natural Science Foundation of China, Grant (No.12175253, No.12027803), the International Partnership Program of the Chinese Academy of Sciences, Grant No.113111KYSB 20190020, the National Key R&D Program of China, Grant No. 2021YFA0718401. The authors acknowledge the HERD PSD colleagues from the INFN and GSSI for the helpful discussions, writing reviews, and editing.

Data availability

Data will be made available on request.

References

[1] D. Kyratzis, On behalf of the H. Collaboration, Overview of the HERD space mission, Phys. Scr. 97 (2022) 054010, https://doi.org/10.1088/1402-4896/ac63fc.
[2] C. Altomare, F. Alemanno, F.C.T. Barbato, P. Bernardini, P.W. Cattaneo, etc, Assembly and test of prototype scintillator tiles for the plastic scintillator detector of the High Energy Cosmic Radiation Detection (HERD) facility, J. Phys. Conf. Ser. 2374 (2022) 012127, https://doi.org/10.1088/1742-6596/2374/1/012127.
[3] R. Bencardino, F. Altaura, V. Bidoli, et al., Response of the LAZIO-SiRad detector to low energy electrons, in: 29th International Cosmic Ray Conference (ICRC29), vol. 2, 2005, p. 449, 2.
[4] Z. Li, Y. Xu, C. Liu, Y. Gu, F. Xie, Y. Li, H. Hu, X. Zhou, X. Lu, X. Li, S. Zhang, Z. Chang, J. Zhang, Z. Xu, Y. Zhang, J. Zhao, Characterization of radiation damage caused by 23MeV protons in Multi-Pixel Photon Counter (MPPC), Nucl. Instrum. Methods Phys. Res. Sect. Accel. Spectrometers Detect. Assoc. Equip. 822 (2016) 63–70, https://doi.org/10.1016/j.nima.2016.03.092.
[5] D. Zhang, X. Li, S. Xiong, Y. Li, X. Sun, Z. An, Y. Xu, Y. Zhu, W. Peng, H. Wang, F. Zhang, Energy response of GECAM gamma-ray detector based on LaBr3:Ce and SiPM array, Nucl. Instrum. Methods Phys. Res. Sect. Accel. Spectrometers Detect. Assoc. Equip. 921 (2019) 8–13, https://doi.org/10.1016/j.nima.2018.12.032.
[6] L.J. Mitchell, B.F. Phlips, J.E. Grove, T. Finne, M. Johnson-Rambert, W.N. Johnson, Strontium iodide radiation instrument (SIRI) – early on-orbit results, in: 2019 IEEE Nucl. Sci. Symp. Med. Imaging Conf. NSSMIC, IEEE, Manchester, United Kingdom, 2019, pp. 1–9, https://doi.org/10.1109/NSS/MIC42101.2019.9059652.
[7] J. Wen, X. Long, X. Zheng, Y. An, Z. Cai, J. Cang, Y. Che, etc, GRID: a student project to monitor the transient gamma-ray sky in the multi-messenger astronomy era, Exp. Astron. 48 (2019) 77–95, https://doi.org/10.1007/s10686-019-09636-w.
[8] A. De Angelis, V. Tatischeff, M. Tavani, U. Oberlack, I. Grenier, etc, the e-ASTROGAM Collaboration, the e-ASTROGAM mission, Exp. Astron. 44 (2017) 25–82, https://doi.org/10.1007/s10686-017-9533-6.
[9] J. McEnery, J.A. Barrio, I. Agudo, M. Ajello, J.-M. Álvarez, S. Ansoldi, Etc, all-sky medium energy gamma-ray observatory: exploring the extreme multimessenger universe. http://arxiv.org/abs/1907.07558, 2019. (Accessed 7 September 2023).
[10] B. Biro, G. David, A. Fenyvesi, J.S. Haggerty, J. Kierstead, E.J. Mannel, T. Majoros, J. Molnar, F. Nagy, S. Stoll, B. Ujvari, C.L. Woody, A comparison of the effects of neutron and gamma radiation in silicon photomultipliers, IEEE Trans. Nucl. Sci. 66 (2019) 1833–1839, https://doi.org/10.1109/TNS.2019.2921102.
[11] G. Lindström, Radiation damage in silicon detectors, Nucl. Instrum. Methods Phys. Res. Sect. Accel. Spectrometers Detect. Assoc. Equip. 512 (2003) 30–43, https://doi.org/10.1016/S0168-9002(03)01874-6.
[12] N. Hirade, H. Takahashi, N. Uchida, M. Ohno, K. Torigoe, Y. Fukazawa, T. Mizuno, H. Matake, K. Hirose, S. Hisadomi, K. Nakazawa, K. Yamaoka, N. Werner, J. Řípa, S. Hatori, K. Kume, S. Mizushima, Annealing of proton radiation damages in Si-PM at room temperature, Nucl. Instrum. Methods Phys. Res. Sect. Accel. Spectrometers Detect. Assoc. Equip. 986 (2021) 164673, https://doi.org/10.1016/j.nima.2020.164673.
[13] K.D. Bartlett, D.D.S. Coupland, D.T. Beckman, K.E. Mesick, Proton irradiation damage and annealing effects in ON Semiconductor J-series silicon photomultipliers, Nucl. Instrum. Methods Phys. Res. Sect. Accel. Spectrometers Detect. Assoc. Equip. 969 (2020) 163957, https://doi.org/10.1016/j.nima.2020.163957.
[14] J.G. Lim, E. Anisimova, B.L. Higgins, J.-P. Bourgoin, T. Jennewein, V. Makarov, Laser annealing heals radiation damage in avalanche photodiodes, EPJ Quantum Technol 4 (2017) 11, https://doi.org/10.1140/epjqt/s40507-017-0064-x.
[15] T. Tsang, T. Rao, S. Stoll, C. Woody, Neutron radiation damage and recovery studies of SiPMs, J. Instrum. 11 (2016), https://doi.org/10.1088/1748-0221/11/12/P12002. P12002–P12002.
[16] T. Tsang, Silicon photomultipliers radiation damage and recovery via high temperature annealing, J. Instrum. 13 (2018), https://doi.org/10.1088/1748-0221/13/10/P10019. P10019–P10019.
[17] M. Calvi, P. Carniti, C. Gotti, C. Matteuzzi, G. Pessina, Single photon detection with SiPMs irradiated up to 1014 cm^{-2} 1-MeV-equivalent neutron fluence, Nucl. Instrum. Methods Phys. Res. Sect. Accel. Spectrometers Detect. Assoc. Equip. 922 (2019) 243–249, https://doi.org/10.1016/j.nima.2019.01.013.
[18] D. Kyratzis, Latest advancements of the HERD space mission, Nucl. Instrum. Methods Phys. Res. Sect. Accel. Spectrometers Detect. Assoc. Equip. 1048 (2023) 167970, https://doi.org/10.1016/j.nima.2022.167970.
[19] M. Kruglanski, N. Messios, E.D. Donder, E. Gamby, S. Calders, L. Hetey, H. Evans, Space Environment Information System (SPENVIS), (n.d.).
[20] Lee Mitchell, Bernard Phlips, W. Neil Johnson, Mary Johnson-Rambert, Anika N. Kansky, Woolf Richard, Radiation damage assessment of SensL SiPMs, Nucl.

Instrum. Methods Phys. Res. Sect. A Accel. Spectrom. Detect. Assoc. Equip. 988 (2021) 164798.
[21] A.R. Altamura, F. Acerbi, B. Di Ruzza, E. Verroi, S. Merzi, A. Mazzi, A. Gola, Radiation damage on SiPMs for space applications, Nucl. Instrum. Methods Phys. Res. Sect. Accel. Spectrometers Detect. Assoc. Equip. 1045 (2023) 167488, https://doi.org/10.1016/j.nima.2022.167488.
[22] M. Moll, Displacement damage in silicon detectors for high energy physics, IEEE Trans. Nucl. Sci. 65 (2018) 1561–1582, https://doi.org/10.1109/TNS.2018.2819506.
[23] Q. An, H.Y. Bai, J. Bao, P. Cao, Y. Chen, etc, Back-n white neutron facility for nuclear data measurements at CSNS, J. Instrum. 12 (2017), https://doi.org/10.1088/1748-0221/12/07/P07022. P07022–P07022.
[24] J. Han, Z. An, G. Zheng, F. Bai, Z. Li, P. Wang, X. Liao, M. Liu, S. Chen, M. Song, J. Zhang, An ion beam facility based on a 3 MV tandetron accelerator in Sichuan University, China, Nucl. Instrum. Methods Phys. Res. Sect. B Beam Interact. Mater. At. 418 (2018) 68–73, https://doi.org/10.1016/j.nimb.2018.01.002.
[25] C. Yi, J. Han, R. Song, X. Yan, F. Ren, X. Luo, Z. Han, C. Wen, G. Qu, X. Liu, W. Lin, P. Wang, Y. Fan, S. Qian, Z. Wang, G. Tang, L. Qin, X. Wang, J. Liu, Discrimination of piled-up neutron-gamma pulses using charge comparison method and neural network for CLYC detectors, Nucl. Instrum. Methods Phys. Res. Sect. Accel. Spectrometers Detect. Assoc. Equip. 1055 (2023) 168561, https://doi.org/10.1016/j.nima.2023.168561.
[26] K.D. Bartlett, D.D.S. Coupland, D.T. Beckman, K.E. Mesick, Proton irradiation damage and annealing effects in ON Semiconductor J-series silicon photomultipliers, Nucl. Instrum. Methods Phys. Res. Sect. Accel. Spectrometers Detect. Assoc. Equip. 969 (2020) 163957, https://doi.org/10.1016/j.nima.2020.163957.
[27] C. Piemonte, A. Ferri, A. Gola, A. Picciotto, T. Pro, N. Serra, A. Tarolli, N. Zorzi, Development of an automatic procedure for the characterization of silicon photomultipliers, in: 2012 IEEE Nucl. Sci. Symp. Med. Imaging Conf. Rec. NSSMIC, IEEE, Anaheim, CA, USA, 2012, pp. 428–432, https://doi.org/10.1109/NSSMIC.2012.6551141.
[28] N. De Angelis, M. Kole, F. Cadoux, J. Hulsman, T. Kowalski, S. Kusyk, S. Mianowski, D. Rybka, J. Stauffer, J. Swakon, D. Wrobel, X. Wu, Temperature dependence of radiation damage annealing of Silicon Photomultipliers, Nucl. Instrum. Methods Phys. Res. Sect. Accel. Spectrometers Detect. Assoc. Equip. 1048 (2023) 167934, https://doi.org/10.1016/j.nima.2022.167934.
[29] H. Liu, Y. Peng, J. Long, W. Lv, K. Liang, R. Yang, D. Han, A technique of in-situ annealing and temperature monitoring for silicon photomultipliers, in: 2019 IEEE Nucl. Sci. Symp. Med. Imaging Conf. NSSMIC, 2019, pp. 1–3, https://doi.org/10.1109/NSS/MIC42101.2019.9059772.